2020 IEEE/RSJ International Conference on Intelligent Robots and Systems (IROS)
October 25-29, 2020, Las Vegas, NV, USA (Virtual)

Robust Micro-Particle Manipulation in a Microfluidic Channel Network Using Gravity-Induced Pressure Actuators

Donghyeon Lee[1], Woongyong Lee[2], Wan Kyun Chung[1], *Fellow, IEEE* and Keehoon Kim[1], *Member, IEEE*

***Abstract*— Robust particle manipulation is a challenging but essential technique for single-cell analysis and processing of microfluidic devices. This paper proposes a micro-particle manipulation system with a microfluidic channel network. We built gravity-induced pressure actuators, which can generate high-resolution output pressure with a wide range so that the multiple particles can be delivered from the inlet of the chip. In this paper, we studied how to model the proposed multi-input-single-output system and sources of disturbances, and designed a robust controller using disturbance observer technique. The performance of the proposed system was verified through experiments.**

I. Introduction

Microfluidic devices are highly integrated system which can conduct various chemical or biological process within a small-size microfluidic chip, and it is a well-known fact that the microfluidic devices have many advantages: fast, accurate and cost-efficient [1], [2]. Especially, many microfluidic devices are widely used to handle micro-particles such as cells, droplets, and microbeads accurately [3]–[6]. To handle micro-particles, various actuation mechanisms have been developed actively, and the techniques are utilized on monitoring, analysis, and drug injection of single cells [7], [8]. Also, there are many studies about single-particle process/analysis methods in passive flow induced by microstructures within the chips [2], [9]

To control the position of the micro-particles in the microfluidic chips, the effective actuation mechanisms have been proposed: electrokinetic effect, acoustic and optical tweezer. The actuation mechanisms have suitable output force resolution (under nN) to manipulate micro-particles, and many research have already shown successful micro-particle control in 2D free space [10].

However, the micro-scale actuation mechanisms are very vulnerable to disturbances due to its limited output range. The actuation easily saturates and loses its control even with the small pressure gradient induced by gravity or surface tension applied to the external reservoirs. Thus, the micro-particle manipulation system requires careful experiment setup to minimize the possible disturbances. Moreover, the actuation effects are easily attenuated with distance, so the

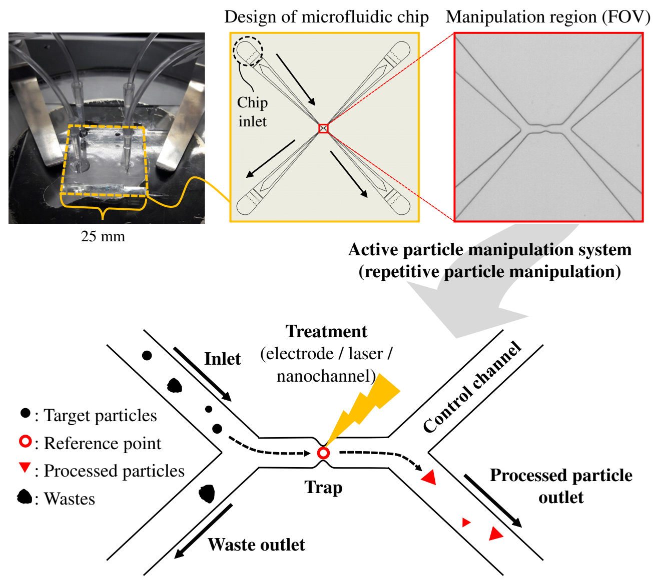

Fig. 1. Repetitive particle manipulation in a microfluidic channel network

manipulable region is strictly limited to a very small area; the target particle should be located within the manipulable region in advance. Such preparation procedure usually takes a long time and large effort; the utility of the micro-particle manipulation techniques is limited from the perspective of the practical applications.

Automating and repeating the micro-particle manipulation process is more challenging than an one-time manipulation experiment. For the robust automation of the micro-particle manipulation, the following requirements should be satisfied.

- The particles should be delivered from the microfluidic chip inlet, which is far from the manipulation region.
- The delivered particle should be accurately controlled (regulated) in the manipulation region.
- The manipulation region should have multiple inlets and outlets to prevent channel clogging due to unexpected large debris and wastes.

For those requirements, the actuation system should have a wide output force range (Fig. 1); the consecutive particle delivery from the chip inlet to the control region requires a large pressure gradient (pressure-induced flow), and the accurate particle control requires small output force resolution.

Beside the actuation output range issue, there is another critical difficulty on the repetitive particle control in the given configuration; the system state is partially observable. In the micro-particle manipulation system, the flowrate and

This research was supported by the Bio & Medical Technology Development Program of the National Research Foundation (NRF) funded by the Ministry of Science and ICT (NRF-2017M3A9F6029736).

[1]The authors are with the Robotics Laboratory, School of Mechanical Engineering, Pohang University of Science and Technology (POSTECH), Pohang, 37673, Gyung-buk, Korea. Email: {sansoveria, wkchung, khk}@postech.ac.kr

[2]The author is with Neuromeka, 06023, Seoul, Korea. Email: woongyong.lee@neuromeka.com

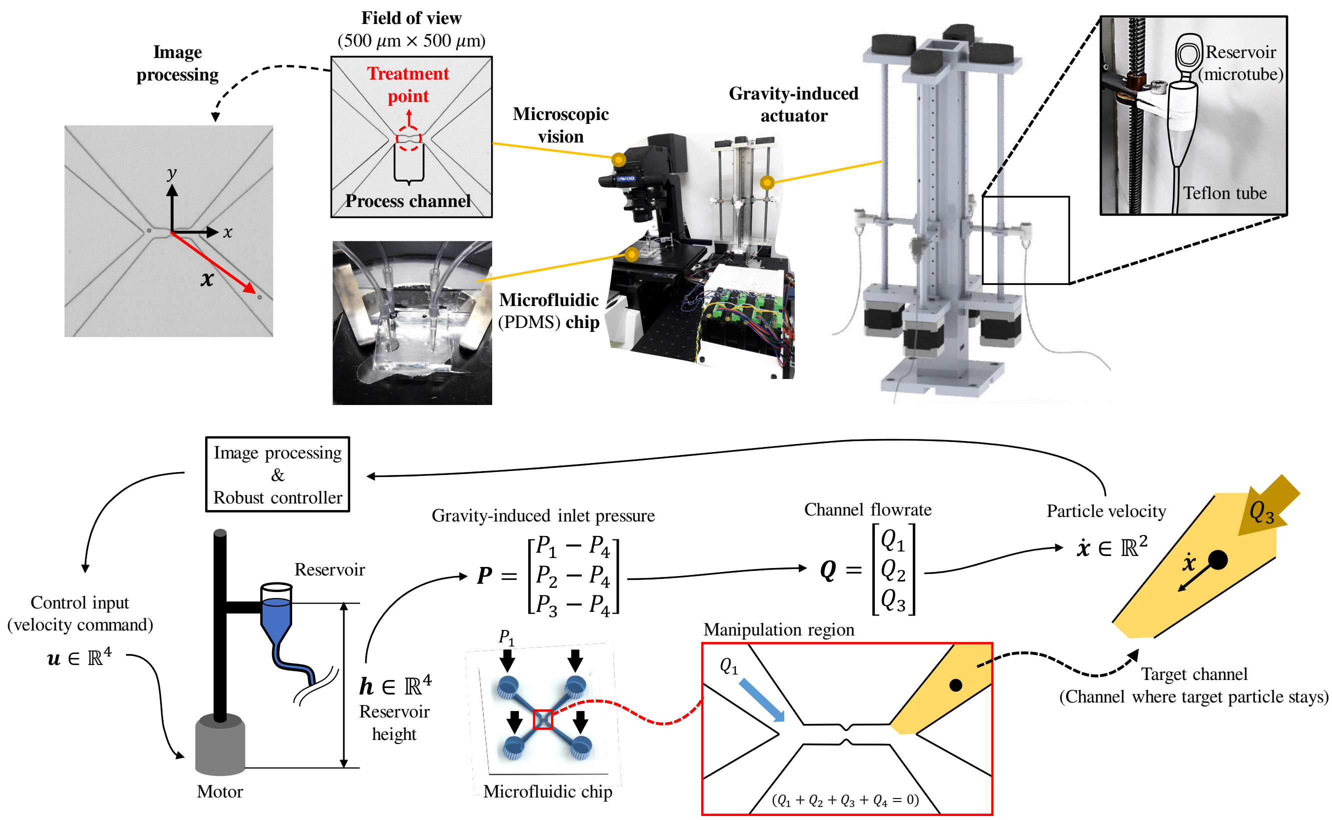

Fig. 2. Configuration of particle manipulation system. The system consists of a microfluidic chip (channel network), gravity-induced pressure actuator, and microscopic vision.

pressure gradient is too weak to be measured with sensors, so the particle movement observed via microscopic vision is the only way to estimate the state of the system. For the microfluidic channel network as shown in Fig. 1, the lack of feedback information becomes more severe because the flowrate or pressure of the channel cannot be measured unless there exist moving particles in the channel. Moreover, in the microfluidic channel network, the motion of the target particle is determined by the combination of the inlet pressure, so the system becomes multi-input-single-output (MISO), which is redundant.

In this study, a systematic solution for repetitive particle manipulation is proposed and empirically validated. We mainly utilized two schemes to deal with the problems mentioned above: the gravitational actuation mechanism and disturbance observer based robust control structure. The gravitational actuation mechanism can generate very fine output (∼100 mPa) while the output range can increase with larger water-level height of the reservoirs [11]. In [11], the authors also suggested in-phase mechanism that can cancel out the mechanical noise from motor and reservoir movement, and we utilized the concept for the manipulation system. Also, the disturbance observer (DOB)-like inner-loop compensator is implemented to compensate for the disturbances. The control procedure specifically targets the automation of the drug injection process introduced in [7], so the sequentially incoming cells (particles) are individually trapped at the treatment point during few seconds and released (Fig. 1).

For simplicity, the major problems dealt in this work can be summarized as below:

- Realization of reasonable actuation output range for both accurate control and repetitive process
- Real-time image processing to distinguish and track the target particle within the FOV
- Planning control rule to handle the redundancy of the microfluidic channel network

The empirical result of the repetitive particle manipulation shows the possibility of the automatic and repetitive single-particle treatment (processing), which can be extended to factory-on-chip for the massive production of the functional particles (cells).

II. System Configuration

This section describes the overall hardware configuration of the proposed particle manipulation system. The system consists of the microfluidic chip (channel network), gravity-induced pressure actuator, and microscopic vision (Fig. 2).

A. Microfluidic channel network

To mimic the particle manipulation environment in [7], we designed a multi-channel network microfluidic chip. The chip is made of polydimethylsiloxane (PDMS) using soft lithography and attached to the slide glass by oxygen plasma bonding. The channel network consists of 5 channels, and the four channels among them are connected to external reservoirs through polymer tubes (Fig. 2). Besides the work in [7], the 5-channel network design is widely used to various functional devices such as sorting, deformability cytometry, and other cellular analysis [4], [12] In the channel network, the center channel work as a process chamber, so the controlled particle is trapped at the treatment point. In [7], the reagent is injected into the cell at the treatment point via an additional nanochannel, which is not configured in this work. The width and length of the center channel is $25\,\mu$m and $100\,\mu$m each, and the overall height of the channel network is approximately $30\,\mu$m.

B. Gravity-induced pressure actuator

The gravity-induced pressure actuation system is developed for repetitive particle manipulation (Fig. 2). The four external reservoirs are connected to the microfluidic chip and open, so the height difference between the reservoirs generates pressure difference due to the gravitational force, and the inlet pressure of each channel can be controlled by moving the reservoirs vertically. Under the assumption that every reservoir has identical shape and surface characteristics, the effect of surface tension at each reservoir is canceled out, so it does not affect the induced pressure gradient inside the microfluidic chip. To control the reservoir height, stepper motors with 8-mm lead linear screws (17HS4401S-M8x8-300MM, Hong Yi Automation Co., China) are used. Lastly, all the actuators are installed on the same base for phase noise cancellation, which minimizes the effect of mechanical vibration of the motor [11].

C. Image acquisition processing for state feedback

As feedback information for the controller, the target particle position is obtained from the microscopic images via image processing algorithm. We used bright-field microscopy (IX-73, Olympus Co., Japan) to acquire images of micro-particle, and the image is captured at 300 fps by a high-speed camera (mvBlueCOURGAR-XD, Matrix vision Co., Germany). The image resolution is 500×500 pixels, and FOV is $500\,\mu m \times 500\,\mu m$.

To extract the position information from acquired images, the following image processing algorithm was applied using the OpenCV library [13]. The background image is subtracted from the current image, and the subtracted image is converted to a binary image by thresholding. Then, the centroid position of each particle can be obtained by using $findContours$ function. Lastly, the particles in the consecutive frames are matched each other, so that the algorithm can track the particle. The Hungarian algorithm is applied to the system to track the moving particles between the consecutive frames. [14].

III. Controller Design

The proposed system is an articulation of various mechanical plants (motor, reservoir, fluid, particle), and the multiple inputs are correlated with each other. Also, some components

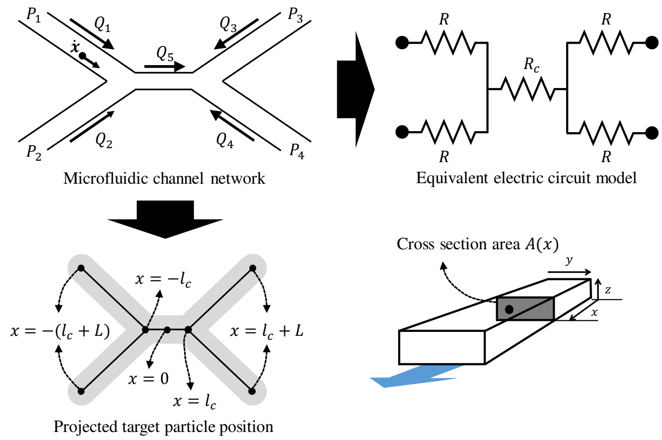

Fig. 3. Modeling of the microfluidic channel network. The channel network (upper left) can be expressed as an equivalent electric circuit (upper right). The 2D position of the particle can be projected on the channel longitudinal direction and expressed with a scalar value (bottom left).

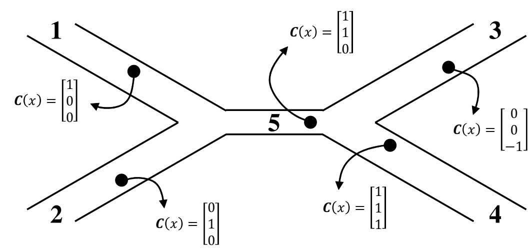

Fig. 4. The channel numbering and channel selection vector $\boldsymbol{C}(x)$ which is determined by the particle position

of the system are nonlinear, so modeling the system plant and applying a model-based controller is effective to control the position of the target particle. In this section, the system is modeled, and a simple PD controller is designed to regulate the particle position. Then, a DOB-based inner-loop compensator is added to the controller to compensate for the errors due to the assumptions made on the system modeling. Lastly, the proposed controller is validated with a numerical simulation, which includes the possible disturbances in the system.

A. System modeling

For the controller design, the microfluidic channel network, gravity-induced pressure actuator are modeled with the assumptions below:

- The particle velocity is the same as the fluid velocity, and the parabolic flow velocity profile can be ignored.
- The compressibility of the fluid and the channel wall can be ignored, and the inertial effect of the fluid can also be ignored.
- The stepper motor has enough bandwidth, so the velocity command input $\boldsymbol{u}$ is directly realized as the motor rotation speed.

From the first assumption, the particle velocity can be obtained directly from the flowrate of the target channel (the channel where the target particle stays). Also, the particle does not move in the lateral direction of the channel, so the 2D particle position $\boldsymbol{x} \in \mathbb{R}^2$ can be expressed with a scalar value x (projected position) by projecting $\boldsymbol{x}$ on the channel longitudinal direction (Fig. 3). Thus, the target particle velocity induced by the flow can be modeled as:

$$\dot{x} = \frac{1}{A(x)}\boldsymbol{C}(x)^\top \boldsymbol{Q}, \tag{1}$$

where $\boldsymbol{Q} = [Q_1, Q_2, Q_3]^\top$ is the flowrate of the fluid inside the inlet channels and $A(x)$ is the area of the cross-section which includes the target particle (Fig. 3). $\boldsymbol{C}(x)$ is the channel selection vector which determines the target channel flowrate from $\boldsymbol{Q}$ and makes the flow direction and the projected particle position coordinate consistent (Fig. 4). In fact, the velocity profile of fluid in a pipe is parabolic, so the fluid velocity is determined with a function of the vertical and lateral position of particle y, z [15]. In this study, the parabolic velocity profile is ignored because the vertical position z is even immeasurable in the current system configuration. The detailed side-effect caused by ignoring the cross-sectional velocity profile of the flow is discussed in the Section V.

With the second assumption, the microfluidic channel network can be modeled, and the relation between the inlet pressure and the flowrate is determined. The microfluidic channel network can be modeled as a simple RLC electric circuit [16]. The conductance and inductance of the microfluidic system can be ignored in the micro-particle manipulation task because fluid is almost incompressible, and the pressure of the microfluidic channels is low. Thus, the channel network can be approximated as an equivalent electric circuit composed of a number of resistors (Fig. 3). The transfer function from the inlet pressure vector $\boldsymbol{P} = [P_1 - P_4, P_2 - P_4, P_3 - P_4]^\top$ to $\boldsymbol{Q}$ can be expressed with a simple constant resistance matrix $\boldsymbol{R}$:

$$\begin{gathered}\boldsymbol{P} = \boldsymbol{R}\boldsymbol{Q}, \\ \text{where } \boldsymbol{R} = \begin{bmatrix} 2R + R_c & R + R_c & R \\ R + R_c & 2R + R_c & R \\ R & R & 2R \end{bmatrix}.\end{gathered} \tag{2}$$

R is the hydrodynamic resistance of the four inlet channels, and R_c is the hydrodynamic resistance of the process channels.

Lastly, the relationship between the motor velocity input $\boldsymbol{u}$, and the inlet pressure $\boldsymbol{P}$ can be determined with the third assumption.

$$\begin{gathered}\boldsymbol{P} = \rho g \begin{bmatrix} 1 & 0 & 0 & -1 \\ 0 & 1 & 0 & -1 \\ 0 & 0 & 1 & -1 \end{bmatrix} \boldsymbol{h} \\ \dot{\boldsymbol{h}} = k\boldsymbol{u},\end{gathered} \tag{3}$$

where ρ is the density of the liquid in the reservoirs, g is the gravitational acceleration, $\boldsymbol{h}$ is the height of the external reservoirs, and k is scale factor from the stepper motor rotor angular position to the linear movement of the lead screw (height change of the reservoirs).

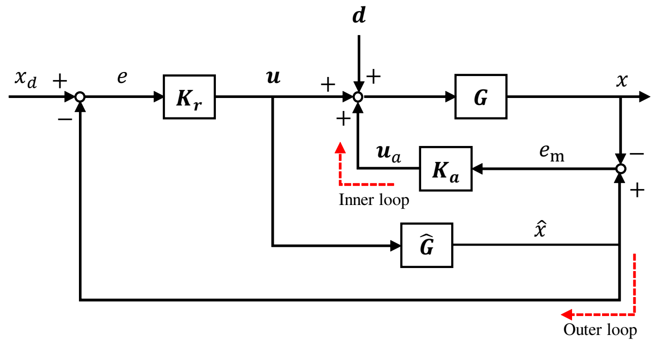

Fig. 5. Block diagram of the proposed controller

In summary, the overall system can be modeled as 2nd-order nonlinear plant :

$$\begin{gathered}\ddot{x} = \frac{\rho g k}{A(x)}\hat{\boldsymbol{G}}(x)\boldsymbol{u}, \\ \text{where } \hat{\boldsymbol{G}}(x) = \boldsymbol{C}(x)^\top \boldsymbol{R}^{-1} \begin{bmatrix} 1 & 0 & 0 & -1 \\ 0 & 1 & 0 & -1 \\ 0 & 0 & 1 & -1 \end{bmatrix}.\end{gathered} \tag{4}$$

B. PD controller for nonlinear MISO system

In designing the controller, there are two issues to be considered: the nonlinearity of the and input redundancy. The nonlinearity of the system can be dealt with linearization of the output signal. From the channel dimension, the cross-sectional area $A(x)$ can be obtained, so the effect can be canceled out by multiplying $A(x)$ to the input.

For the input redundancy, a heuristic control rule is proposed. The controller for the MISO system should generate a multi-dimensional vector (control input $\boldsymbol{u}$) from the scalar value observation. For the redundant problem, there exist many schemes such as least square. In this problem, the solution may be obtained by calculating the pseudo-inverse of $\boldsymbol{G}_n(x)$, but the channel selection vector $\boldsymbol{C}(x)$ is highly nonlinear, so it easily induces instability like chattering when the particle moves near the junction of the channels. Thus, a constant input weight vector $\boldsymbol{C}_r$ is used to determine $\boldsymbol{u}$:

$$\mathbf{C}_r = \begin{bmatrix} 0.5 \\ 0.5 \\ -0.5 \end{bmatrix}. \tag{5}$$

By using $\boldsymbol{R}\boldsymbol{C}_r$ instead of the pseudo-inverse of $\hat{\boldsymbol{G}}(x)$, a simple PD controller can be designed as:

$$\boldsymbol{u} = \boldsymbol{K}_r(e) = (k_r e + k_d \dot{e})\frac{A(x)}{\rho g k}\mathbf{R}\mathbf{C}_r, \tag{6}$$

where k_r is the gain of the proportional controller, and k_d is the gain of the derivative controller.

C. DOB-based inner-loop compensator

The designed PD controller can control the particle only when there are no disturbances. The disturbances and unmodeled force always exist in the microfluidic system, so it is necessary to compensate for the disturbances. Thus, the

DOB-based inner-loop compensator is designed to reject the disturbances in the system.

In the general DOB structure for linear systems, the control input is estimated by using the inverse of the model plant $\hat{\boldsymbol{G}}^{-1}$ and designing proper Q filter. By subtracting the estimated control input and the real control input, the disturbance can be estimated, and it is added to the control input. However, the DOB structure cannot be directly applied to the proposed system because it is nonlinear and redundant, so the DOB structure is slightly modified following the work in [17] (Fig. 5). In [17], it is shown that the modified structure can extend the concept of the DOB into the nonlinear system (it even enhance the robust stability of the system). In the modified structure, the ideal particle velocity $\dot{\hat{x}}$ is obtained by using the model $\hat{\boldsymbol{G}}$ instead of using the inverse of the model plant. Then, the real output and the estimated output is compared, and the error between the two value e_m is compensated with the auxiliary compensator $\boldsymbol{K}_a$:

$$\boldsymbol{u}_a = \boldsymbol{K}_a(e_m) = \left(k_a + k_i \int edt\right) \frac{A(x)}{\rho g k} \mathbf{R}\mathbf{C}_a(x), \quad (7)$$

where k_a is the gain of the proportional controller, and k_i is the gain of the integral controller.

The inner-loop compensator $\boldsymbol{K}_a$ has a very similar structure with the outer-loop controller $\boldsymbol{K}_r$ (the PD controller in the previous section) because they share the nonlinearity and redundancy problem of the system. The difference between the $\boldsymbol{K}_r$ and $\boldsymbol{K}_{\boldsymbol{a}}$ is that the PI controller is used to the compensator to remove the constant bias (disturbance), which induces the non-vanishing error, and the input weight vector $\boldsymbol{C}_a$ is determined with the different rules. Assuming a particle is in channel i, e_m can be reduced by giving the input weight as:

$$\mathbf{C}_{a,j}(x) = \begin{cases} \frac{\sqrt{3}}{2} & \text{if } i = j \\ -\frac{\sqrt{3}}{6} & \text{if } i \neq j \end{cases} \quad (8)$$

(if particle x is in channel $j \neq 5$),

$$\mathbf{C}_a(x) = \begin{bmatrix} 0.5 \\ 0.5 \\ -0.5 \end{bmatrix} \quad (9)$$

(if particle x is in channel $j = 5$).

By using this rule, the particle asymptotically follows the ideal plant behavior in channel i.

D. Simulation of the proposed controller

To test the feasibility of the controller, the numerical simulation is performed. The forward Euler method is used to simulate the plant behavior with a timestep of $100\,\mu$s, while the control loop frequency is 20 Hz. The simulated plant includes the time delay due to the motor dynamics (the motor dynamics is modeled as a 1st-order low pass filter) Also, the possible disturbances (including model uncertainty and unmodeled dynamics) are analyzed as below and implemented to the simulated plant.

First, the inconsistent image processing (position noise) can induce the particle position error (Fig. 6a). The next issue

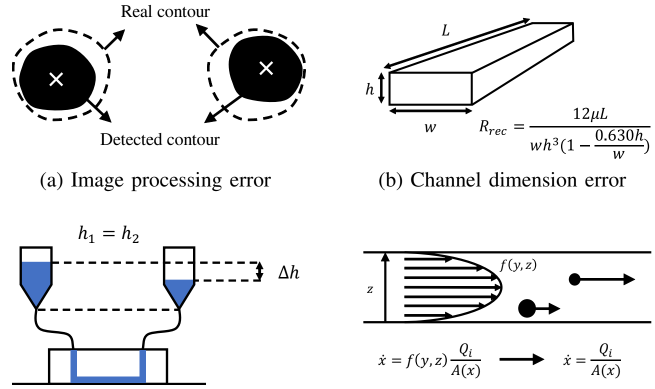

Fig. 6. Modeling of disturbance and effect of parameter uncertainties in the micro-particle manipulation system

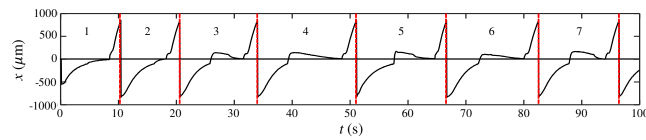

Fig. 7. Simulation result of the repetitive particle manipulation process

is the uncertainty of the channel dimension (Fig. 6b). When we design a controller, the parameters like hydrodynamic resistance are determined based on the system model, but micro-scale fabrication is often inaccurate. For microfluidic channels, even a small error in the channel height dimension can make a huge error in the hydraulic resistance of the channel. Thirdly, the reservoir height (the encoder measurement) is not the actual height of the liquid-air interface, so the bias occurs on the control input (Fig. 6c). Lastly, the ignored nonlinear velocity profile of the flow amplifies or reduces the plant output (Fig. 6d).

For each particle, the analyzed disturbances are set as random values. In the simulation, the target particle is manipulated to the center of channel 5 (the treatment point), and the position regulation is considered as ”success” if the particle stays at the treatment (the center of channel 5) more than 1 s. Then, the reference point of the control is changed to the endpoint of channel 4 so that the processed particle is released. After the processed particle leaves the FOV, the system increases the pressure of the channel 1 and waits for the new particle. As a result of the simulation, 7 micro-particles are successfully controlled within 100 s (Fig. 7). Actually, it cannot be guaranteed that the model used in the numerical simulation is identical to the real micro-particle manipulation system because the fabricated chip dimension can be different from the model. Also, there are many more unmodeled factors that can affect the manipulation system, such as temperature and surface tension, so it is hard to expect the result of the simulation would be identical to the real experiment. However, the simulation shows that the implemented controller, which includes the robust inner-loop compensator, can compensate for the disturbance modeled in

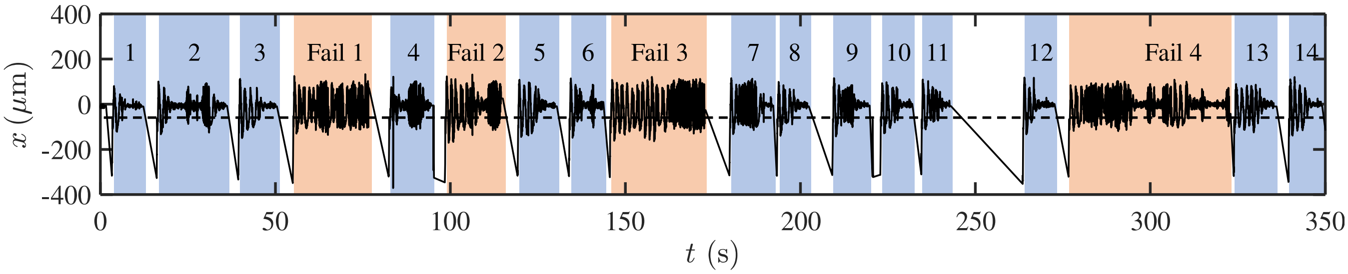

(a) Position of the target particles during the repetitive particle manipulation process. 14 particles are successfully controlled among 18 particles.

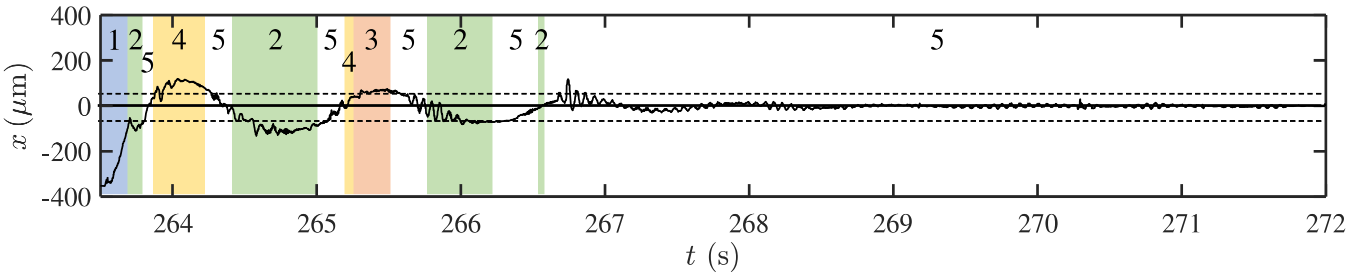

(b) Particle behavior of the successful case. The colored shadow and number means the channel where the particle stays.

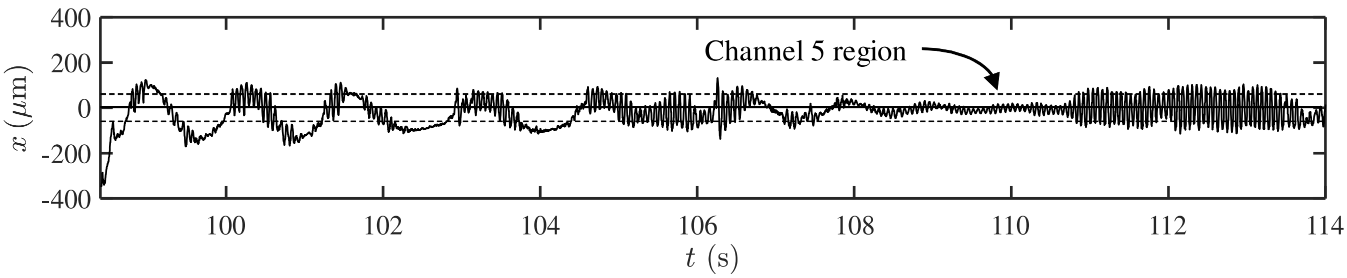

(c) Particle behavior of the failed case. The vibration is not attenuated until the particle removed from the FOV.

Fig. 8. Experiment result of the repetitive micro-particle manipulation

the simulation. In the following experiment result section, the failure cases are also shown during the manipulation, and the reason for the failure is discussed in Section V.

IV. Experiment Result

The repetitive micro-particle manipulation is performed with the proposed system. To perform the repetitive task, the controller waits for a particle to enter the FOV with predefined input (high pressure at channel 1 and low pressure at the other channels). When a particle enters the FOV, the controller begins to regulate the position of the particle and moves the particle to the reference point. If the particle is stabilized at the origin, release command is given to the controller manually (clicking interface button), then the predefined control input is given to the actuators to get rid of the particle (low pressure at channel 4 and high pressure at the other channels). After the particle leaves the FOV, the controller rolls back the actuators to the first state, and wait for a new particle.

During 350 s, 14 particles were successfully controlled to be processed, and 4 particles were failed to be stabilized (Fig. 8a). The particle delivery to the reference point and stabilization took a similar time to the simulation result, which was near 10 s per particle, but the particles showed more unstable behavior near the process channel. In the unstable situation, the particle traveled between the channels more. Due to such instability, 4 particles could not be stabilized for a long time, so the released button is clicked manually, and the particles are released.

The clue for the instability can be found by comparing the target position trajectory of the successful and failed case. In the successful case, the particle is stabilized gradually, traveling between the channels like the simulation result (Fig. 8b). The oscillating behavior notably increases when the target particle is in the channel 5 (process channel). However, the larger oscillation is seen in the failed case (Fig. 8c). The interesting fact is that the oscillation problem got alleviated, and the particle control was stabilized right after the unstable particle is released. More detailed discussions on the instability will be presented in Section V.

Additionally, a longer experiment is performed to ensure the robust performance of the proposed manipulation system. In the supplementary video, the repetitive particle manipulation video is shown. Totally 43 trials are performed to control the individual particles, and the 32 particles are successfully manipulated during 625 s.

V. Discussion

In this paper, the particle manipulation system is proposed for the repetitive cell drug injection process. The developed gravity-induced pressure actuator could generate a wide range of output pressure; it could generate enough pressure gradient to deliver the particles from the chip inlet, which is far from FOV (manipulation region) and also accurately regulate the particle position with the small output resolution. Also, the double-loop control structure could successfully stabilize the incoming particles and showed robust particle control performance under various disturbances, even with inaccurate modeling. Especially, the environment factors such as temperature, reservoir surface condition (ripple, water-level) can affect the behavior of the system, but they are almost impossible to be modeled. In the experiment shown in the supplementary video, the overall success rate is 74%, which is not much high. However, the system can be said "robust" because the experiment condition (especially unmodeled disturbance) continuously changes during the experiment.

In the experiments, there are three types of failure cases. The first type is due to the excessive system instability. From the fact that the large oscillation occurs only for the specific particles in the experiment, the parabolic velocity profile of the fluid can be suspected as the cause of the instability. Each incoming particle locates at a different height in the channel, and it changes the scale between the flowrate and particle velocity. Therefore, the particle shows divergent motion more easily if its vertical position is near the center of the channel. In the manipulation system, the four vertical actuators share their base to cancel out the mechanical noise (in-phase system in [11]). However, small vibration remains as shown in Fig.8b and 8c, and the effect of vibration can be more severe if the particle locates the center of the channel.

The second failure type is missing particles due to its excessive incoming velocity. Because the newly incoming particles are at outside of FOV, we do not have control on the velocity of the particles before they enter FOV. Some particles have very high velocity when it enters FOV, and the system cannot regulate the particle due to the limited bandwidth. The missed particle easily escape the FOV, and the system waits for the new particle to enter the FOV.

The last failure type is due to the sinking/sticking problem. Because the PDMS channel wall has sticky surface, so the particles easily stick to the wall during manipulation. Also, some particles sink at the bottom of the chip when they are too slow. In such situation, the particle does not move with small pressure gradient (flow), so it is better to flush it away with large flowrate (release the particle).

Therefore, the following future work would be to reduce the above failure cases. In order to remove the instability due to the excessively high speed, other actuation mechanisms can be combined with the gravity-induced actuator. Specifically, the piezo actuators have a fast response; it would be an effective solution to enhance the stability and performance of the system, as shown in [18]. Also, the sampling rate of the visual feedback (high-speed camera) is a critical bottleneck of the overall control performance, so implementing a faster camera would be a effective solution to increase the success rate of the process.

At the current stage, the throughput of the experiment result is extremely low, but the proposed manipulation system shows the possibility of the active micro-particle manipulation systems for the massive particle process, and the upcoming development of the actuation system will extend the use of active micro-particle manipulation framework.

References

[1] D. N. Breslauer, P. J. Lee, and L. P. Lee, "Microfluidics-based systems biology," *Molecular Biosystems*, vol. 2, no. 2, pp. 97–112, 2006.

[2] J. Nilsson, M. Evander, B. Hammarström, and T. Laurell, "Review of cell and particle trapping in microfluidic systems," *Analytica chimica acta*, vol. 649, no. 2, pp. 141–157, 2009.

[3] P. Novo, M. Dell'Aica, D. Janasek, and R. P. Zahedi, "High spatial and temporal resolution cell manipulation techniques in microchannels," *Analyst*, vol. 141, no. 6, pp. 1888–1905, 2016.

[4] X. Wang, S. Chen, M. Kong, Z. Wang, K. D. Costa, R. A. Li, and D. Sun, "Enhanced cell sorting and manipulation with combined optical tweezer and microfluidic chip technologies," *Lab on a Chip*, vol. 11, no. 21, pp. 3656–3662, 2011.

[5] D. Wong and C. L. Ren, "Microfluidic droplet trapping, splitting and merging with feedback controls and state space modelling," *Lab on a Chip*, vol. 16, no. 17, pp. 3317–3329, 2016.

[6] Y.-C. Tan, K. Hettiarachchi, M. Siu, Y.-R. Pan, and A. P. Lee, "Controlled microfluidic encapsulation of cells, proteins, and microbeads in lipid vesicles," *Journal of the American Chemical Society*, vol. 128, no. 17, pp. 5656–5658, 2006.

[7] C.-K. Yun, J. W. Hwang, T. J. Kwak, W.-J. Chang, S. Ha, K. Han, S. Lee, and Y.-S. Choi, "Nanoinjection system for precise direct delivery of biomolecules into single cells," *Lab on a Chip*, vol. 19, no. 4, pp. 580–588, 2019.

[8] S. Sakuma, K. Kuroda, C.-H. D. Tsai, W. Fukui, F. Arai, and M. Kaneko, "Red blood cell fatigue evaluation based on the close-encountering point between extensibility and recoverability," *Lab on a Chip*, vol. 14, no. 6, pp. 1135–1141, 2014.

[9] H. Tavakoli, W. Zhou, L. Ma, S. Perez, A. Ibarra, F. Xu, S. Zhan, and X. Li, "Recent advances in microfluidic platforms for single-cell analysis in cancer biology, diagnosis and therapy," *TrAC Trends in Analytical Chemistry*, 2019.

[10] R. Probst, Z. Cummins, C. Ropp, E. Waks, and B. Shapiro, "Flow control of small objects on chip: Manipulating live cells, quantum dots, and nanowires," *IEEE Control Systems*, vol. 32, no. 2, pp. 26–53, 2012.

[11] K. Mizoue, M. H. Phan, C.-H. D. Tsai, M. Kaneko, J. Kang, and W. K. Chung, "Gravity-based precise cell manipulation system enhanced by in-phase mechanism," *Micromachines*, vol. 7, no. 7, p. 116, 2016.

[12] J. S. Dudani, D. R. Gossett, T. Henry, and D. Di Carlo, "Pinched-flow hydrodynamic stretching of single-cells," *Lab on a Chip*, vol. 13, no. 18, pp. 3728–3734, 2013.

[13] G. Bradski, "The OpenCV Library," *Dr. Dobb's Journal of Software Tools*, 2000.

[14] H. W. Kuhn, "The hungarian method for the assignment problem," *Naval Research Logistics (NRL)*, vol. 2, no. 1-2, pp. 83–97, 1955.

[15] Y. J. Heo, J. Kang, M. Kaneko, and W. K. Chung, "A hybrid actuator system for single particle manipulation on a microfluidic chip," in *Robotics and Automation (ICRA), 2015 IEEE International Conference on*. IEEE, 2015, pp. 2691–2697.

[16] Y. J. Heo, J. Kang, M. J. Kim, and W. K. Chung, "Tuning-free controller to accurately regulate flow rates in a microfluidic network," *Scientific reports*, vol. 6, p. 23273, 2016.

[17] M. J. Kim, Y. Choi, and W. K. Chung, "Bringing nonlinear $\mathcal{H}_\infty$ optimality to robot controllers," *IEEE Transactions on Robotics*, vol. 31, no. 3, pp. 682–698, 2015.

[18] K. Mizoue, N. Yagyu, C.-H. D. Tsai, and M. Kaneko, "Hybrid actuation for long-term cell manipulation in a microfluidic channel," in *2017 IEEE International Conference on Advanced Intelligent Mechatronics (AIM)*. IEEE, 2017, pp. 1089–1094.